Effects of Conversion of Phenylalanine-31 to Leucine on the Function of Human Dihydrofolate Reductase†

Neal J. Prendergast,‡ James R. Appleman,§ Tavner J. Delcamp,‡ Raymond L. Blakley,§,‖ and James H. Freisheim*,‡

Department of Biochemistry, Medical College of Ohio, CS 10008, Toledo, Ohio 43699, Department of Biochemical and Clinical Pharmacology, St. Jude Children's Research Hospital, Memphis, Tennessee 38101, and Department of Pharmacology, University of Tennessee College of Medicine—Memphis, Memphis, Tennessee 38163

Received November 29, 1988; Revised Manuscript Received February 23, 1989

ABSTRACT: Oligonucleotide-directed, site-specific mutagenesis was used to convert phenylalanine-31 of human recombinant dihydrofolate reductase (DHFR) to leucine. This substitution was of interest in view of earlier chemical modification studies (Kumar et al., 1981) and structural studies based on X-ray crystallographic data (Matthews et al., 1985a,b) which had implicated the corresponding residue in chicken liver DHFR, Tyr-31, in the binding of dihydrofolate. Furthermore, this particular substitution allowed testing of the significance of protein sequence differences between mammalian and bacterial reductases at this position with regard to the species selectivity of trimethoprim. Both wild-type (WT) and mutant (F31L) enzymes were expressed and purified by using a heterologous expression system previously described (Prendergast et al., 1988). Values of the inhibition constants (K_i values) for trimethoprim were 1.00 and 1.08 μM for WT and F31L, respectively. Thus, the presence of phenylalanine at position 31 in human dihydrofolate reductase does not contribute to the species selectivity of trimethoprim. The K_m values for nicotinamide adenine dinucleotide phosphate (reduced) (NADPH) and dihydrofolate were elevated 10.8-fold and 9.4-fold, respectively, for the mutant enzyme, whereas the V_{max} increased only 1.8-fold. Equilibrium dissociation constants (K_D values) were obtained for the binding of NADPH and dihydrofolate in binary complexes with each enzyme. The K_D for NADPH is similar in both WT and F31L, whereas the K_D for dihydrofolate is 43-fold lower in F31L. Values for dihydrofolate association rate constants (k_{on}) with enzyme and enzyme–NADPH complexes were measured by stopped-flow techniques. These values are $(3.5 \pm 0.8) \times 10^8$ M^{-1} s^{-1} (F31L) and $(2.2 \pm 0.3) \times 10^8$ M^{-1} s^{-1} (WT) with enzyme alone and $(0.5 \pm 0.1) \times 10^8$ M^{-1} s^{-1} (F31L) and $(1.5 \pm 0.2) \times 10^8$ M^{-1} s^{-1} (WT) with enzyme·NADPH. On the basis of these alterations in the interaction of dihydrofolate with F31L when compared to wild type, we conclude that Phe-31 functions directly in substrate binding to apoenzyme under equilibrium conditions as well as to enzyme forms occurring during steady-state catalytic cycling.

Dihydrofolate reductase (DHFR)[1] (5,6,7,8-tetrahydrofolate:$NADP^+$ oxidoreductase, EC 1.5.1.3) is an enzyme essential for the growth and replication of cells. DHFR catalyzes the nicotinamide adenine dinucleotide phosphate (reduced) (NADPH)[1]-dependent reduction of dihydrofolate (H_2F)[1] to tetrahydrofolate (H_4F),[1] a process necessary for the continuation of purine, pyrimidine, and nucleotide biosynthesis. Inhibitors of this enzyme, most notably the anti-folate compounds methotrexate (MTX)[1] and trimethoprim (TMP),[1] are used extensively in clinical settings for the treatment of neoplastic and infectious disorders. Trimethoprim is a particularly potent antibacterial agent capable of producing 50% inhibition of *Escherichia coli* DHFR at concentrations 30 000–60 000 times lower than needed to produce the same effect on human (h)[1] DHFR (Burchall & Hitchings, 1965; Li et al., 1982).

The molecular basis for the species selectivity of DHFR inhibition by TMP has been extensively reviewed (Matthews et al., 1985a,b; Birdsall et al., 1983). Using refined X-ray structural data from chicken liver (clDHFR)[1] and *E. coli* DHFR complexed with TMP, Matthews and co-workers observed two potential binding sites for the 3,4,5-trimethoxybenzyl moiety of TMP in both DHFR species, designated the "upper" and "lower" clefts. For each DHFR, the inhibitor trimethoxybenzyl moiety occupies a different position (upper cleft in clDHFR and lower cleft in *E. coli* DHFR) (Matthews et al., 1985a,b). The consequences of this altered side-chain conformation in clDHFR (and presumably all vertebrate DHFRs) is a repositioning of the 2,4-diaminoheterocycle component of TMP such that a critical H bond is lost between the carbonyl oxygen of Val-115 and the 4-amino group of the 2,4-diaminoheterocycle (Matthews et al., 1985b). The explanation offered by Matthews and his colleagues for the orientation of the benzyl side chain of TMP in an "up" conformation in vertebrate reductases was because of the significantly increased width across the cavity bounded by helices αB and αC observed in clDHFR along with the presence of Tyr at position 31 (instead of Leu-28 in *E. coli* DHFR). Consequently, the benzyl side chain of TMP cannot be favorably accommodated in the lower cavity of clDHFR as

† This work was supported in part by USPHS Research Grants R01 CA41461 (to J.H.F.) and R01 CA31922 (to R.L.B.), by Cancer Center Core Grant P30 CA 21765 (to R.L.B.) from the National Cancer Institute, National Institutes of Health, and by American Lebanese Syrian Associated Charities (to R.L.B. and J.R.A.).

* Correspondence should be addressed to this author.
‡ Medical College of Ohio.
§ St. Jude Children's Research Hospital.
‖ University of Tennessee College of Medicine–Memphis.

[1] Abbreviations: MTX, methotrexate (4-amino-10-methyl-4-deoxyfolic acid); TMP, trimethoprim [2,4-diamino-5-(3,4,5-trimethoxybenzyl)pyrimidine]; hDHFR, human dihydrofolate reductase; clDHFR, chicken liver dihydrofolate reductase; H_2F, dihydrofolic acid; H_4F, tetrahydrofolic acid; SDS, sodium dodecyl sulfate; PAGE, polyacrylamide gel electrophoresis; $NADP^+$, nicotinamide adenine dinucleotide phosphate (oxidized); NADPH, nicotinamide adenine dinucleotide phosphate (reduced); Tris-HCl, tris(hydroxymethyl)aminomethane hydrochloride.

0006-2960/89/0428-4645$01.50/0

demonstrated by model-building experiments (Matthews et al., 1985b).

Recently, however, this hypothesis has been challenged by Oefner and co-workers, who examined the crystal structure of hDHFR complexed with folate (Oefner et al., 1988). These authors argued that the increase in width across the lower cavity in the human enzyme is hardly significant, thus concluding that the explanation of the altered conformation of TMP in clDHFR is not valid for the human enzyme.

Vertebrate enzymes conserve an aromatic residue at position 31 (Tyr or Phe) whereas leucine is found at the corresponding position in *E. coli* and *Lactobacillus casei* DHFRs (Freisheim & Matthews, 1984). In an attempt to determine the significance of this structural difference between vertebrate and bacterial DHFRs regarding TMP selectivity, Phe-31 of hDHFR was replaced with leucine by oligodeoxynucleotide-directed mutagenesis. Furthermore, this particular substitution allowed us to test previous predictions from this laboratory, extrapolated from chemical modification studies on clDHFR (Kumar et al., 1981), regarding the role of Phe-31 in H_2F binding.

Experimental Procedures

Materials. Synthetic oligodeoxynucleotides were prepared on an Applied Biosystems Model 380A automated DNA synthesizer. Methotrexate, NADPH, and $NADP^+$ were purchased from Sigma. Dihydrofolate was prepared from folic acid by the method of Blakley (1960). Trimethoprim was a generous gift from Dr. David Baccanari of Burroughs-Wellcome. Restriction endonucleases, T4 polynucleotide kinase, and T4 DNA ligase were purchased from Bethesda Research Laboratories.

Mutagenesis and DNA Sequencing. F31L was generated by the method of Inouye and Inouye (1987), which utilizes double-stranded plasmid DNA as the template for oligodeoxynucleotide-directed mutagenesis. A 22-mer oligodeoxynucleotide (5′-CAGGAATGAATTCAGATATTTC-3′) containing one mismatch (shown underlined) from the WT sequence in the expression plasmid pDFR (Prendergast et al., 1988) was used to convert Phe-31 → Leu by this method. Following transformation of the bacterial host JM101 with the mutagenesis reaction mixture, bacteria were plated onto LB agar plates containing 50 μg/mL ampicillin. Isolation of F31L from WT plasmid was accomplished by colony hybridization analysis using the ^{32}P-labeled oligodeoxynucleotide shown above. Prehybridization and hybridization conditions used in these experiments were determined as described by Inouye and Inouye (1987). DNA sequence analysis of the entire coding region of F31L was performed as previously described (Prendergast et al., 1988).

Expression and Purification of hDHFRs. Both WT and F31L were expressed from a procaryotic high-level expression vector previously described (Prendergast et al., 1988). Homogeneous, ligand-free WT and F31L hDHFRs were prepared as previously described (Prendergast et al., 1988).

Enzyme Assays and Initial Velocity Studies. DHFR activity was measured spectrophotometrically at 22 °C in 50 mM Tris-HCl (pH 7.5) unless otherwise indicated. The assay monitors a decrease in absorbance at 340 nm which occurs when NADPH and H_2F are converted to $NADP^+$ and H_4F. The molar extinction coefficient for the reaction at 340 nm is 12 300 (Hillcoat et al., 1967). Measurements of K_m values for NADPH and H_2F were performed as previously described (Delcamp et al., 1983; Prendergast et al., 1988). Although progress curves were obtained as described previously, the calculation of the K_m for H_2F with wild-type hDHFR was carried out as described by Appleman et al. (1988a) for DHFR from *Escherichia coli*. Analysis of initial velocity data was performed with a computer program which uses nonlinear least-squares analysis (Cleland, 1967). Measurements of K_i values for $NADP^+$ and TMP were made from initial velocity experiments and calculated as described in the legend for Table IV.

Determination of K_i for H_4F. The H_4F K_i value for F31L was calculated from full time courses of the enzymic reaction at 20 °C where the concentration of NADPH upon initiation and throughout the entire reaction is both saturating and in large excess of $NADP^+$ at any given time. This ensures that the measured inhibition reflects the presence of H_4F and minimizes any contribution by $NADP^+$. The rate of disappearance of H_2F is described by

$$\frac{d[H_2F]}{dt} = -\frac{V_{max}[H_2F]_t}{[H_2F]_t + K_m(1 + [H_4F]_t/K_i)}$$

where K_m is the Michaelis constant for H_2F, V_{max} is the rate of product formation at saturating substrate concentrations, $[H_2F]_t$ and $[H_4F]_t$ are the concentrations of H_2F and H_4F at time t after initiation of catalysis, and K_i is the inhibition constant for H_4F. Since $[H_4F]_t = [H_2F]_i - [H_2F]_t$, where $[H_2F]_i$ is the initial $[H_2F]$, then

$$\frac{d[H_2F]}{dt} = -\frac{V_{max}[H_2F]_t}{[H_2F]_t + K_m[(1 + [H_2F]_i - [H_2F]_t)/K_i]}$$

The solution of this differential equation and best-fit values of V_{max} and K_i were calculated by using the program CRICF described by Chandler et al. (1972). The value of K_m was described in separate experiments (see above) and held constant at 0.30 μM.

Determination of K_i for MTX. The K_i values for MTX were calculated from the dependence of steady-state enzyme activity at 20 °C on inhibitor concentration as described previously (Appleman et al., 1988a). Enzymes were preincubated with NADPH and MTX, and H_2F was added to this reaction mixture. Initially, the reaction velocity is small, but it gradually increases until a constant reaction rate (i.e., steady-state rate) is reached.

Determination of Equilibrium Dissociation Constants (K_D Values). Dissociation constants for the interactions of ligands with both WT and F31L enzymes were determined by titrating the change in enzyme fluorescence that accompanies enzyme-ligand complex formation at 20 °C. Procedures and calculations for the determination of the NADPH K_D were as described previously (Appleman et al., 1988a). For the determination of the K_D for the H_2F binding, independent mixtures of enzyme and H_2F were prepared at each H_2F concentration (rather than serial addition of H_2F to a single enzyme solution) due to the instability of H_2F over the long times involved in serial titration. In the calculation of the values for K_D for both NADPH and H_2F, the concentration of enzyme was treated as a parameter, and best-fit values of both K_D and enzyme concentration were determined. It should be noted that the K_D values calculated in this fashion were in good agreement with values from calculations in which the enzyme concentration was held constant at the value determined by titration with the tight-binding inhibitor MTX.

Determination of H_2F Association Rate Constants (k_{on}). Values of k_{on} for formation of binary enzyme·H_2F complexes were determined at 20 °C in stopped-flow experiments, as described for MTX binding to *E. coli* DHFR (Appleman et al., 1989; Beard et al., 1989). The intensity of intrinsic protein fluorescence at 340 nm was measured through a band-pass

Table I: Dissociation Constants (K_D Values) and Fluorescence Quenching Properties of hDHFRs[a]

enzyme	K_D (nM)		max % quench	
	NADPH	H_2F	NADPH	H_2F
WT	10.3 ± 3.4	52 ± 16	71	74
F31L	6.7 ± 1.2	1.2 ± 0.9	73	81
F31L/WT	0.65	0.023		

[a] Protein was excited at 280 nm, and protein fluorescence emission was monitored at 340 nm.

filter from Corion Corp. Complex formation was monitored by the quenching of the fluorescence accompanying H_2F binding to the enzyme.

The value of k_{on} for H_2F binding to form the ternary complex, enzyme·NADPH·H_2F, for each enzyme was determined in single-turnover experiments. The rate of conversion of enzyme-bound substrates to enzyme-bound products is extremely fast (Appleman et al., 1988b, 1989), and the equilibrium strongly favors product formation so that when low concentrations of H_2F are mixed with an excess of hDHFR·NADPH, the reaction scheme may be treated as

$$\text{enzyme·NADPH} + H_2F \xrightarrow{k_{on}} \text{enzyme·NADP}^+\text{·}H_4F$$

The time course of formation of $NADP^+$ and H_4F is monitored by the decrease in absorbance at 340 nm accompanying conversion of substrate to product when H_2F is mixed with enzyme·NADPH in a stopped-flow spectrophotometer. The value of k_{on} was calculated by fitting this time course to equations appropriate for a second-order reaction using nonlinear least-squares techniques (Appleman et al., 1988a).

Results and Discussion

Oligonucleotide-directed, site-specific mutagenesis was used to introduce leucine in place of phenylalanine at position 31 in hDHFR. The entire coding region of the mutant DHFR, F31L, was determined by double-stranded dideoxy sequence analysis. The results verified the correct substitution of Phe-31 → Leu and demonstrated that no other alteration in the hDHFR cDNA coding region had occurred. Both wild type (WT) and F31L were expressed in *E. coli* from an expression plasmid previously described (Prendergast et al., 1988), and both DHFRs were purified to homogeneity as determined by sodium dodecyl sulfate–polyacrylamide gel electrophoresis (SDS–PAGE)[1] (data not shown).

Affinity labeling studies using a ^{14}C-labeled 4,6-diaminodihydrotriazine bearing a terminal benzenesulfonyl fluoride (DTBSF) have implicated Tyr-31 as an active-site residue in clDHFR (Kumar et al., 1981). These authors demonstrated a direct correlation between loss of enzymatic activity and labeling of Tyr-31 with DTBSF. Furthermore, simultaneous incubation with NADPH did not protect clDHFR from inactivation by DTBSF whereas incubation with H_2F did. These results suggested that Tyr-31 forms part of the H_2F binding domain in clDHFR. The results presented below demonstrate that the corresponding residue (Phe-31) in hDHFR also appears to function as a part of the H_2F binding domain.

Dissociation constants (K_D values) for NADPH and H_2F in binary complexes with both mutant and WT DHFRs have been determined (Table I). NADPH binding showed little variation between WT and F31L, whereas the H_2F binding properties were altered dramatically, with H_2F binding 43-fold tighter to the mutant enzyme as compared to wild type.

It may be shown that $K_D = k_{off}/k_{on}$ where the bimolecular association of hDHFR with H_2F is opposed by a unimolecular dissociation reaction, and where k_{on} and k_{off} are the rate constants governing these reactions. The increased affinity of F31L for H_2F could therefore reflect an increase in k_{on}, a decrease in k_{off}, or a combination of these factors when compared to wild-type enzyme. Values of k_{on} for the association reaction for each enzyme are indicated in Table II. Although this value is somewhat greater for F31L than for WT, the 1.6-fold increase cannot explain the far greater difference in K_D values. The rate at which H_2F is released from hDHFR must therefore be much slower for F31L than for WT. Values of k_{off} could not be accurately determined by the procedures used, but from the values of k_{on} and K_D for each enzyme, k_{off} should be 27-fold smaller for the mutant enzyme than for wild type. An alternate possibility that is currently under investigation is that the increased affinity of the mutant enzyme for H_2F is the result of an isomerization of the enzyme–H_2F complex formed during the initial association reaction that is more favorable for F31L than for WT. Such an isomerization has been observed upon MTX binding to WT hDHFR, but not upon TMP binding to this enzyme (Appleman et al., 1988b). Whether the increased affinity is a consequence of altered values of k_{off} or changes in the equilibrium between enzyme·H_2F conformers, the alteration in this active-site residue clearly has a much greater effect on the interaction of H_2F with hDHFR after complex formation than it does upon that rate at which the hDHFR·H_2F complex is formed.

Table II: Dihydrofolate Association Rate Constants (k_{on} Values) for hDHFRs (M^{-1} s^{-1})

enzyme	binary[a]	ternary[b]	binary/ternary
WT	(2.2 ± 0.3) × 10^8	(1.5 ± 0.2) × 10^8	1.5
F31L	(3.5 ± 0.8) × 10^8	(0.5 ± 0.1) × 10^8	7
F31L/WT	1.6	0.33	

[a] For binding of H_2F to hDHFR. [b] For binding of H_2F to enzyme·NADPH.

Table III: Steady-State Properties of hDHFRs

enzyme	Michaelis constants (μM)		V_{max} (s^{-1})
	NADPH	H_2F	
WT	0.26 ± 0.04	0.032 ± 0.002	7.4 ± 0.22
F31L	2.8 ± 0.6	0.30 ± 0.03	13.4 ± 0.7
F31L/WT	10.8	9.4	1.8

Some steady-state kinetic parameters for F31L and WT hDHFR are compared in Table III. The catalytic coefficient (V_{max}) and Michaelis constant (K_m) for H_2F are elevated 1.8- and 9.4-fold, respectively. In principle, values of steady-state parameters such as these can be predicted from rate constants for the individual steps in the reaction pathway as has been done previously for other enzymes. We have therefore measured values of the association rate constant k_{on} for H_2F binding to enzyme–NADPH complexes as described under Experimental Procedures (Table II). These values are calculated from time courses of product formation in single-turnover experiments with WT and F31L hDHFR like those depicted in Figure 1.

Values for all of the various association and dissociation constants for substrates and products, the forward and reverse rate constants for hydride transfer, and the kinetic sequence involved in catalysis derived from these constants were first reported for DHFR from *Escherichia coli* by Fierke et al. (1987). When the concentration of NADPH is much greater than its K_m, the Scheme I describes the predominant pathway during catalytic cycling for this DHFR where the symbols are as follows: E, DHFR; NH, NADPH; H_2F, dihydrofolate; N, $NADP^+$; H_4F, tetrahydrofolate, k's, rate constants. At neutral pH and at saturating concentrations of NADPH, the rate-

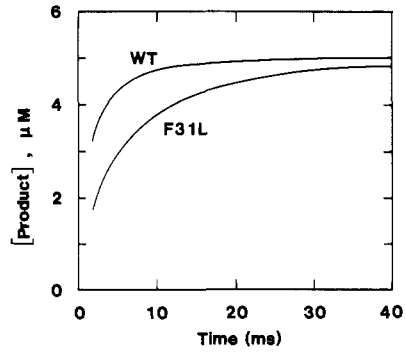

FIGURE 1: Time courses of product formation from single turnovers of WT and F31L human DHFR. Each enzyme was preincubated with NADPH and mixed with H_2F in stopped-flow measurements. Enzyme concentrations were 6.3 and 5 μM for WT and F31L human DHFR, respectively. NADPH concentration was 100 μM. H_2F concentration was 5 μM. For these concentrations of reactants, binding of H_2F is rate limiting in the formation of the products $NADP^+$ and H_4F. Reactions are so fast that a substantial portion of each reaction time course is lost in the instrumental dead time.

Scheme I

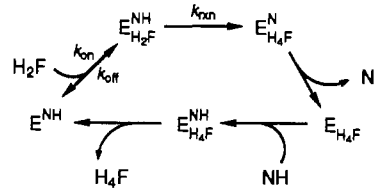

limiting step in catalysis is release of H_4F from the E·NADPH·H_4F complex. Under these conditions, the overall rate for the reaction sequence E·NADPH·H_4F → → → E·NADPH is much greater than that for E·$NADP^+$·H_4F → E·NADPH·H_2F (Fierke et al., 1987). Therefore, it may be shown that the K_m for H_2F equals $V_{max}(k_{rxn} + k_{off})/k_{on}k_{rxn}$ where k_{rxn} governs the pH-dependent rate of conversion of enzyme-bound substrates to products (E·NADPH·H_2F → E·$NADP^+$·H_4F). For both WT and F31L hDHFR, k_{rxn} is very large at neutral pH (Appleman et al., 1989; Beard et al., 1989) and is probably much larger than k_{off}, the rate constant governing H_2F release from E·NADPH·H_2F. Therefore, the value of the K_m for H_2F should be equal to V_{max}/k_{on} if the catalytic sequence for these enzymes is like that for DHFR from *E. coli*. For F31L hDHFR, the directly measured value of 0.30 μM is in excellent agreement with the value of 0.27 μM calculated from the appropriate value of V_{max} in Table III and k_{on} in Table II (=13.4 $s^{-1}/0.5 \times 10^8$ M^{-1} s^{-1}). Similarly, the K_m for H_2F with WT is 0.032 μM, and the ratio of rate constants equals 0.049 μM. Currently ongoing investigations into the kinetic sequence of catalysis under somewhat different experimental conditions indicate that the sequence of steps in the catalytic cycle is indeed like those depicted above for F31L hDHFR but that this scheme is insufficient to completely describe the behavior of WT hDHFR. Therefore, the reasonably good agreement between the directly measured value of K_m and the ratio of V_{max}/k_{on} with WT may be fortuitous. It is interesting to note that the value of K_D for H_2F binding to WT (0.052 μM) is approximately equal to the H_2F K_m in WT (0.032 μM), whereas the H_2F K_D and K_m differ by more than 2 orders of magnitude in F31L (0.0012 and 0.30 μM, respectively).

It was surprising that the K_m for NADPH is increased as much as that for H_2F by the amino acid substitution Phe-31 → Leu (Table III). Differences in the sequence of steps in the catalytic cycle for WT versus F31L hDHFR could explain the 10.7-fold increase in the K_m for NADPH, as could alterations in the interaction of NADPH with ternary complexes of hDHFR, NADPH, and either H_2F or H_4F. Alternatively, the NADPH binding domain might be directly affected by the amino acid substitution although it is believed that residue 31 in hDHFR does not interact with NADPH. Also, it may be seen from the NADPH K_D values in Table I that the tightness of binding of this ligand has not been altered by replacement of Phe-31 with Leu, so that gross perturbations of the NADPH binding site are highly unlikely.

Table IV: Inhibition Constants (K_i Values) for hDHFRs

	compound			
enzyme	TMP[a] (μM)	MTX (pM)	H_4F (μM)	$NADP^+$[a] (μM)
WT	1.00 ± 0.09	0.51 ± 0.02	[b]	0.74 ● 0.07
F31L	1.08 ± 0.04	0.33 ± 0.07	0.37 ± 0.06	1.78 ± 0.30
F31L/WT	1.08	0.65		2.41

[a] Values of K_i for $NADP^+$ and TMP were calculated by fitting the dependence of steady-state velocity on concentration of inhibitor and competing substrate (H_2F for TMP and NADPH for $NADP^+$). [b] As discussed in the text and shown in Figure 2, the presence of H_4F leads to an increase in activity with WT.

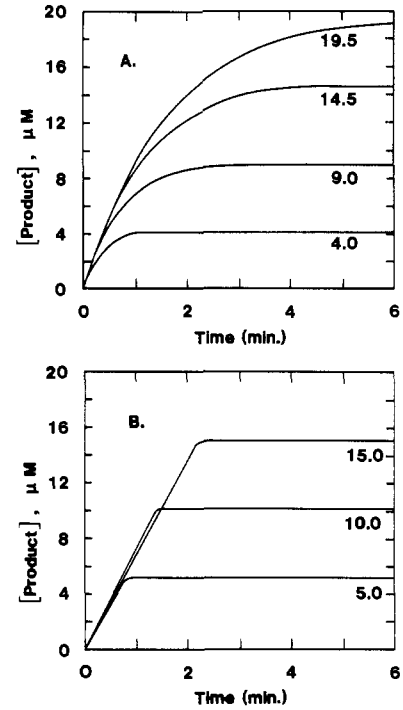

FIGURE 2: Full time courses of the catalytic reaction for F31L and WT human DHFR. In each progress curve, the enzyme concentration was 10 nM, and the NADPH concentration was 100 μM. H_2F concentrations for each curve are shown in the figure. (Panel A) Time courses obtained with F31L human DHFR are depicted. The curves generated from the best-fit values of V_{max} and K_i for H_4F were indistinguishable from the experimental values. For additional details, see Experimental Procedures. (Panel B) Time courses obtained with WT human DHFR. Since it was not practical to determine values of K_i for H_4F, only the experimentally determined values are shown.

Values of the inhibition constants (K_i) for the reaction products $NADP^+$ and H_4F are found in Table IV. $NADP^+$ is only slightly less inhibitory for F31L hDHFR than for WT, and is a classical competitive inhibitor with respect to NADPH with both enzymes. Conversely, inhibition by H_4F is quite different for the two enzymes. Progress curves were obtained for each enzyme under conditions designed to measure inhibition by H_4F as described under Experimental Procedures. As shown in Figure 2, panel A, the activity of F31L hDHFR decreases substantially as H_4F accumulates. The value of K_i for H_4F for this enzyme was calculated from these progress

curves and is equal to 0.37 μM. The time courses of product formation catalyzed by WT enzyme contrast strikingly with these results, since in this case the catalytic rate actually increases slightly as H_4F accumulates. This is demonstrated by the slight increase in slope with time for each progress curve with WT hDHFR (Figure 2, panel B) and only decreases when almost all of the substrate H_2F has been depleted. How the substitution of Leu for Phe-31 leads to such a change in behavior is unclear, but one might speculate that this residue could influence the rate of H_4F release which, in the case of *E. coli* enzyme, has been shown to be almost completely rate limiting under the conditions used in these experiments (Fierke et al., 1987).

Inhibitor constants for the anti-folate compounds MTX and TMP have been determined for both WT and F31L (Table IV). It has been established for hDHFR that TMP behaves as a classical competitive inhibitor with regard to H_2F (Appleman et al., 1988b). Substitution with leucine at position 31 does not alter this pattern (data not shown). Trimethoprim K_i values for both WT and F31L are shown in Table IV and are nearly identical. Given the small difference in the TMP K_i values between WT and F31L, these results demonstrate that the substitution of Phe-31 → Leu does not significantly impact on TMP's ability to inhibit the enzyme. If one reviews the initial hypothesis put forth regarding the stereochemical features of clDHFR that distinguish its TMP binding properties from *E. coli* DHFR, the results obtained with F31L are not completely unexpected. It has been postulated that a widening in the lower cleft of clDHFR prevents Tyr-31 (or Phe-31 in other vertebrate DHFRs) from providing favorable hydrophobic contacts with TMP similar to those provided by Leu-28 in the *E. coli* enzyme (Matthews et al., 1985b). Recently, however, reports on the X-ray structure of hDHFR have rejected the relevance of this hypothesis to TMP binding in hDHFR based on the finding that the width across the lower cavity is similar to that seen in the *E. coli* enzyme (Oefner et al., 1988). Therefore, one might be tempted to conclude that the sole reason for the inability of TMP to bind to hDHFR in a conformation like that in *E. coli* DHFR is due to steric hindrance attributable to Phe-31. In this case, replacement of Phe-31 with Leu should have allowed TMP to bind in the "down" conformation and presumably result in much tighter binding to this mutant enzyme. However, TMP binds equally tightly to either WT or F31L. We believe that this indicates that the inhibitor side chain binds in the upper cleft in both of these enzymes, although X-ray crystallographic studies are required to ensure that this interpretation is correct. This finding, although significant in that it rules out one key structural distinction between hDHFR and bacterial DHFRs (as related to TMP species selectively), leaves open the question as to what differences in binding site features are responsible. Additional mutagenesis experiments on both *E. coli* and human DHFRs should help to clarify this issue.

Both F31L and WT were strongly inhibited by MTX, with K_i values in both enzymes ranging in low picomolar levels. It is interesting to note that while only minor changes were observed in the inhibitor binding properties of F31L for both TMP and MTX, significant changes were seen for both H_2F and H_4F. Particularly noteworthy is the difference in binding of MTX versus H_2F under steady-state conditions. As indicated in Table IV, MTX inhibition is increased very slightly in F31L over WT where H_2F, in contrast, is a much poorer substrate (the K_m for H_2F is 9.4-fold larger in F31L versus WT). This suggests that Phe-31 interactions with H_2F are different from those with MTX. This notion is consistent with X-ray structural reports on the orientation of MTX with hDHFR (Oefner et al., 1988) which show the pteridine ring of MTX to be in an inverse orientation relative to the folate binding conformation.

In summary, we have used site-directed mutagenesis to begin exploring structure–function relationships in hDHFR. This study addresses the role of Phe-31 in the kinetic and binding properties of this enzyme. It is clear that this residue forms part of the H_2F binding domain as determined by the significant changes in H_2F and H_4F binding properties associated with substituting this residue with leucine. In contrast, the NADPH binding and catalytic properties of this mutant suggest that Phe-31 does not form contacts with NADPH necessary for binding or hydride ion transfer. This is consistent with X-ray reports on clDHFR and hDHFR which do not place Phe-31 (or Tyr-31) in the NADPH binding pocket. The presence of this aromatic residue in hDHFR at this position does not appear to contribute to the species selectivity of TMP. Finally, comparison of substrate versus inhibitor binding properties, determined from solution studies, demonstrates distinct binding differences between MTX and H_2F within the active site of the enzyme.

ACKNOWLEDGMENTS

We thank Kevin Rodeman for excellent technical assistance and Dr. Manohar Ratnam for his helpful suggestions. We also thank Ann Chlebowski for preparing the manuscript. During the course of this work, use was made of the Harold and Helen McMaster Recombinant DNA Laboratory.

Registry No. MTX, 59-05-2; TMP, 738-70-5; hDHFR, 9002-03-3; H_2F, 12592-22-2; H_4F, 135-16-0; NADP, 53-59-8; NADPH, 53-57-6; Phe, 63-91-2; leucine, 61-90-5.

REFERENCES

Appleman, J. R., Howell, E. E., Kraut, J., Kühl, M., & Blakley, R. L. (1988a) *J. Biol. Chem. 263*, 9187–9198.

Appleman, J. R., Prendergast, N. J., Delcamp, T. J., Freisheim, J. H., & Blakley, R. L. (1988b) *J. Biol. Chem. 263*, 10304–10313.

Appleman, J. R., Beard, W. A., Delcamp, T. J., Prendergast, N. J., Freisheim, J. H., & Blakley, R. L. (1989) *J. Biol. Chem. 264*, 2625–2633.

Beard, W. A., Appleman, J. R., Delcamp, T. J., Freisheim, J. H., & Blakley, R. L. (1989) *J. Biol. Chem.* (in press).

Birdsall, B., Roberts, G. C. K., Feeney, J., Dann, J. G., & Burgen, A. S. V. (1983) *Biochemistry 22*, 5597–5604.

Blakley, R. L. (1960) *Nature (London) 188*, 231–232.

Burchall, J. J., & Hitchings, G. H. (1965) *Mol. Pharmacol. 1*, 126–136.

Chandler, J. P., Hill, D. E., & Spivey, H. O. (1972) *Comput. Biomed. Res. 5*, 515–534.

Cleland, W. W. (1967) *Adv. Enzymol. Relat. Areas Mol. Biol. 29*, 1–32.

Delcamp, T. J., Susten, S. S., Blankenship, D. T., & Freisheim, J. H. (1983) *Biochemistry 22*, 633–639.

Fierke, C. A., Johnson, K. A., & Benkovic, S. J. (1987) *Biochemistry 26*, 4085–4092.

Freisheim, J. H., & Matthews, D. A. (1984) in *Folate Antagonists as Therapeutic Agents* (Sirotnak, F. M., Burchall, J. J., Ensminger, W. D., & Montgomery, J. A., Eds.) Vol. 1, pp 69–131, Academic Press, Orlando, FL.

Hillcoat, B. L., Nixon, P. F., & Blakley, R. L. (1967) *Anal. Biochem. 21*, 178–189.

Inouye, S., & Inouye, M. (1987) in *DNA and RNA Synthesis* (Narang, S., Ed.) Academic Press, Orlando, FL.

Kumar, A. A., Mangum, J. H., Blankenship, D. T., &

Freisheim, J. H. (1981) *J. Biol. Chem. 256*, 8970–8976.
Li, R. L., Hansch, C., Matthews, D. A., Blaney, J. M., Langridge, R., Delcamp, T. J., Susten, S. S., & Freisheim, J. H. (1982) *Quant. Struct.-Act. Relat. Pharmacol., Chem. Biol. 1*, 1–7.
Matthews, D. A., Bolin, J. T., Burridge, J. M., Filman, D. J., Volz, K. W., Kaufman, B. T., Beddel, C. R., Champness, J. N., Stammers, D. K., & Kraut, J. (1985a) *J. Biol. Chem. 260*, 381–391.
Matthews, D. A., Bolin, J. T., Burridge, J. M., Filman, D. J., Volz, K. W., & Kraut, J. (1985b) *J. Biol. Chem. 260*, 392–399.
Oefner, C., D'Arcy, A., & Winkler, F. K. (1988) *Eur. J. Biochem. 174*, 377–385.
Penner, M. H., & Frieden, C. (1985) *J. Biol. Chem. 260*, 5366–5369.
Prendergast, N. J., Delcamp, T. J., Smith, P. L., & Freisheim, J. H. (1988) *Biochemistry 27*, 3664–3671.
Stone, S. R., & Morrison, J. F. (1982) *Biochemistry 21*, 3757–3765.

Structure–Activity Relationships in the Hydrolysis of Substrates by the Phosphotriesterase from *Pseudomonas diminuta*†

William J. Donarski, David P. Dumas, David P. Heitmeyer, Vincent E. Lewis, and Frank M. Raushel*
Department of Chemistry, Texas A&M University, College Station, Texas 77843
Received October 18, 1988; Revised Manuscript Received December 16, 1988

ABSTRACT: The mechanism and substrate specificity of the phosphotriesterase from *Pseudomonas diminuta* have been examined. The enzyme hydrolyzes a large number of phosphotriester substrates in addition to paraoxon (diethyl *p*-nitrophenyl phosphate) and its thiophosphate analogue, parathion. The two ethyl groups in paraoxon can be changed to propyl and butyl groups, but the maximal velocity and K_m values decrease substantially. The enzyme will not hydrolyze phosphomonoesters or -diesters. There is a linear correlation between enzymatic activity and the pK_a of the phenolic leaving group for 16 paraoxon analogues. The β value in the corresponding Brønsted plot is −0.8. No effect on either V_{max} or V_{max}/K_m is observed when sucrose is used to increase the relative solvent viscosity by 3-fold. These results are consistent with rate-limiting phosphorus–oxygen bond cleavage. A plot of log V versus pH for the hydrolysis of paraoxon shows one enzymatic group that must be unprotonated for activity with a pK_a of 6.1. The deuterium isotope effect by D_2O on V_{max} and V_{max}/K_m is 2.4 and 1.2, respectively, and the proton inventory is linear, which indicates that only one proton is "in flight" during the transition state. The inhibition patterns by the products are consistent with a random kinetic mechanism.

Over 30 million kilograms of organophosphorus pesticides are used annually in the United States (FAO, 1983). The usefulness of these compounds is due to their inhibition of acetylcholinesterase in insects. This is also the primary cause of toxicity in nontarget organisms—including man. Exposure to excess levels of organophosphorus compounds not only has immediate consequences but has been shown to exert delayed cholinergic toxicity (Abou-Donia et al., 1979; Ali & Fukuto, 1983) and delayed neurotoxicity (Metcalf, 1982). Smart (1987) has shown organophosphorus residues could be found in fresh vegetables and fruits taken from grocers throughout Europe, and Muhammad and Kawar (1985) have shown parathion to be present in ketchup 6 months after processing. Thus, an enzyme capable of hydrolyzing paraoxon (diethyl *p*-nitrophenyl phosphate), parathion (diethyl *p*–nitrophenyl thiophosphate), and several other related organophosphorus compounds (Scheme I) is of scientific as well as environmental value. One such enzyme was reported by Munnecke (1976), but the enzymatic mechanism of this phosphotriesterase has only recently been studied.

Scheme I

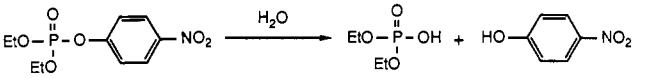

Paraoxon

Lewis et al. (1988) demonstrated that the phosphotriesterase from *Pseudomonas diminuta* would only hydrolyze the S_P isomer of the common pesticide ethyl *p*-nitrophenyl phenylthiophosphonate (EPN) and that this hydrolysis occurred through the inversion of stereochemistry at phosphorus. These results suggest a general base mechanism for the activation of a water molecule and the subsequent nucleophilic attack by the oxygen directly at the phosphorus center. A phosphoenzyme intermediate in this reaction mechanism is highly unlikely because of the net inversion of configuration (Knowles, 1980).

This paper further details some aspects of the enzymatic hydrolysis mechanism of the *Ps. diminuta* phosphotriesterase. The proton-transfer process and the participation of the putative active-site base are probed through the measurement of solvent deuterium isotope effects and an analysis of the effects of pH on the kinetic parameters V_{max} and V_{max}/K_m. A systematic variation of the leaving group ability of substituted phenols and the effect of solvent viscosity on the kinetic parameters are used to elucidate the rate-limiting step and

†This work was supported in part by the Army Research Office (DAAL03-87-K-0017), the Robert A. Welch Foundation (A-840), and the Texas Advanced Technology Program. F.M.R. is the recipient of NIH Research Career Development Award DK-01366.
* Address correspondence to this author.

0006-2960/89/0428-4650$01.50/0